Calculation and controlled factors of hydrocarbon expulsion efficiency using corrected pyrolysis parameters: A Songliao case study

Haitao Xue[1], Zhentao Dong[1], Shansi Tian[2*], Shuangfang Lu[1], Hugh Christopher Greenwell[3], Peng Luo[3], Wenhua Zhang[2], Shudong Lu[5], Min Wang[1], Wei Ma[6,7], Yifeng Wang[6,7]

[1] School of Geosciences, China University of Petroleum (East China), Qingdao 266580, Shandong, PR China

[2] Key Laboratory of continental shale hydrocarbon accumulation and efficient development (Northeast Petroleum University), Ministry of Education, Northeast Petroleum University, Daqing, 163318, Heilongjiang, PR China

[3] Department of Earth Science, Durham University, Durham， DH1 3LE, United Kingdom

[4] Energy Division, Saskatchewan Research Council, Saskatchewan, S4S 7J7, Canada,

[5] Richfit Information Technology Co., Ltd. CNPC，Beijing, 100000，China

[6] Langfang Branch of PetroChina Research Institute of Petroleum Exploration & Development, Langfang 065007, China

[7] Key Laboratory of Gas Reservoir Formation and Development, CNPC, Langfang 065007, China

Corresponding authors:
Shansi Tian
Phone (or Mobile) No.: +86-18661904371
Email: shan.tian@nepu.edu.cn

ABSTRACT

In recent years, rock pyrolysis parameters combined with a mass balance method have been used to calculate the hydrocarbon expulsion efficiency. However, due to the experimental procedure of rock pyrolysis, the residual hydrocarbon amount (S_1) is underestimated, and the hydrocarbon-generation potential of kerogen (S_2) is overestimated, so that the hydrocarbon expulsion efficiency calculated from the pyrolysis parameters before correction is higher than the actual value. In this paper, the pyrolysis parameters were corrected by performing pyrolysis before and after the extraction of source rocks, and the hydrocarbon expulsion efficiency of the mudstone of the Qing 1 member of the Ha14 well in Songliao basin was calculated using the chemical kinetics method. The hydrocarbon expulsion efficiencies before and after the correction were considerably different, the hydrocarbon expulsion efficiency of the Ha14 well after correction was 17.5% lower than that before correction. The study show that the higher the abundance and maturity of source rock are, the higher the hydrocarbon expulsion efficiency is; the oil-type organic matter has a higher hydrocarbon-expulsion efficiency than the gas-type organic matter; the interbedded sand and mud type source-reservoir configuration relationship is beneficial to hydrocarbon expulsion; the underwater diversion channel phase has the highest hydrocarbon expulsion efficiency.

Keywords: hydrocarbon expulsion efficiency; recovery of original hydrocarbon-generation potential; pyrolysis parameters correction; chemical kinetics

1 INTRODUCTION

Oil and gas can only contribute to the accumulation in a conventional reservoir after being expelled from the source rock. The process of hydrocarbon movement out of the source rock is the hydrocarbon expulsion. While exploring hydrocarbon, numerous questions come in the mind of petroleum geologists, viz. When are oil and gas expelled from the source rock? What amount is expelled, and in what phase? What geological regularity is observed in the process of transport? Compared with numerous methods used to study hydrocarbon generation, the evaluation of hydrocarbon expulsion remains limited, and hydrocarbon expulsion efficiency can only be obtained after the above questions are properly addressed. The analysis and calculation of hydrocarbon expulsion efficiency in each period of hydrocarbon migration has essential theoretical and practical significance viz. quantitative evaluation of hydrocarbon source rocks, relatively accurate calculation of oil and gas resources, and the subsequent prediction of the pattern of oil and gas distribution (Liu et al., 2017; Liu et al., 2019).

Nowadays, some progress has been made in understanding the mechanism driving force of primary migration, the time and depth of hydrocarbon expulsion, the mode and phases of transport, hydrocarbon expulsion efficiency, and hydrocarbon expulsion amount (Li et al., 2020; Ma et al., 2020; Pandey et al., 2018; Singh et al., 2016a; Singh P.K., 2012; Singh et al., 2016b; Singh et al., 2017a; Singh et al., 2017b; Wang et al., 2020), but a weak link remains in petroleum geology research in understanding the relationship between the latter.

The hydrocarbon expulsion efficiency (HEE) of source rock is the proportion of the hydrocarbons that have been expelled relative to generated (Dickey, 1975), and is controlled by the amount of hydrocarbons generated from the source rock and the source rock residual hydrocarbon capacity. The amount of generated hydrocarbons in a source rock is mainly affected by the abundance, type, and maturity of the organic matter, the temperature, and the type of minerals present that contribute to the organic matter conversion catalysis (Li et al., 2015). The residual hydrocarbon amount of the source rock itself is influenced not only by the above three factors but also by temperature (Lafargue et al., 1990), formation pressure (Wu et al., 2016), rock structure (porosity and permeability) (Zeng et al., 2021), lithology, and the formation fluid's physical properties (Milliken et al., 2020).

For evaluating the hydrocarbon expulsion efficiency, numerous research methods have been developed, including the residual hydrocarbon method (Leythaeuser et al., 1984) , multi-phase flow theory (Ungerer et al., 1990), hydrocarbon saturation method (Sandvik et al., 1992), geological analogy (White and Gehman, 1979), thermal simulation experiments of hydrocarbon generation, and expulsion (Behar et al., 1992;

Behar et al., 1995; Blanc and Connan, 1992; Landais et al., 1994; Lewan, 1997; Lewan et al., 2014; Li et al., 2008; Rullkötter et al., 1988; Sweeney et al., 1995), original hydrocarbon generation potential recovery method, evolution trend surface subtraction, hydrocarbon generation potential method (Lafargue et al., 1990; Lafargue et al., 1994; Li et al., 2008; Ungerer et al., 1990; Varma et al., 2015), and the mass balance method (Leythaeuser et al., 1987). Each method has disadvantages (Li et al., 2015). For example, the geological temperatures of hydrocarbon expulsion process generally lower than 70°C. However, thermal simulation experimental methods need high temperature condition (generally higher than 300°C) to study hydrocarbon expulsion. Hence, the experimental results are not convincing for some scholars.

Hydrocarbon expulsion models, such as the compaction model and multiple phase flow model (Dickey, 1975; Leythaeuser et al., 1984) , can be built to simulate the hydrocarbon generation and expulsion of source rocks in the laboratory (Behar et al., 1992; Behar et al., 1995; Blanc and Connan, 1992; Lafargue et al., 1990; Lafargue et al., 1994; Landais et al., 1994; Lewan, 1997; Lewan et al., 2014; Li et al., 2008; Rullkötter et al., 1988; Sandvik et al., 1992; Sweeney et al., 1995; Ungerer et al., 1990; White and Gehman, 1979) or to analyze and calculate the hydrocarbon expulsion efficiency using actual geological and geochemical data (Dembicki Jr et al., 1983; Huang et al., 2017; Jiang, et al., 2010; Xie et al., 2014). Currently, there are many uncertainties and disagreements in the understanding of the dynamics, phases, channels, and modes of hydrocarbon expulsion. There are significant differences between hydrocarbon expulsion measured in the laboratory environment and hydrocarbon expulsion under geological conditions (Chen et al., 2015). Different experimental conditions (Li et al., 2018) will result in differences in the hydrocarbon expulsion efficiency calculated using a model and the value obtained from experimental simulations.

In recent years, the generation and expulsion mechanism of source rocks has been combined with the principle of mass balance, and routinely obtained geochemical data, such as TOC (Total Organic Carbon), S_1 (Hydrocarbon generation in unit mass oil rock at 300℃), S_2 (Hydrocarbon generation in unit mass oil rock at 300℃-600℃), Ro (Vitrinite Reflectance Ratio), have been used to calculate the hydrocarbon expulsion efficiency (Li et al., 2015). However, since S_1 and S_2 in the pyrolysis data pertaining to geochemical information do not fully represent the residual hydrocarbons in the source rock and the residual hydrocarbon-generation potential of kerogen, the calculated amount of generated hydrocarbon and the residual hydrocarbon amount are inaccurate, which has a significant impact on the calculation of the hydrocarbon expulsion efficiency.

This paper seek to correct the pyrolysis parameters (S_1, S_2) of source rocks to calculate hydrocarbon expulsion efficiency and analysis its controlled factors. In section 2.1, the geological background and sample information of the study area were given in detail. In section 2.2-2.3, the incorrect use of the pyrolysis parameters in the calculation of the hydrocarbon expulsion efficiency was analyzed, and then, the pyrolysis parameters of source rocks was corrected by comparing the pyrolysis parameters before and after the extraction. In Section 2.4, the model for calculating the hydrocarbon expulsion efficiency was developed, moreover, the key parameters F (hydrocarbon generation conversion rate) was recovered by hydrocarbon generation kinetics. In Section 2.5, the improved ΔlogR technique was used for modeling with hydrocarbon expulsion efficiency. In Section 3, the influence of source rock organic abundance, type, maturity, source rock thickness, source-reservoir configuration relationship, and sedimentation relative hydrocarbon expulsion efficiency was analyzed.

2 METHODOLOGY

2.1 Geological Background and Sample Information

The target horizons are the Qingshankou Formation (K_2qn_1 and $K_2qn_{2\text{-}3}$) in the northern Songliao Basin. The Late Cretaceous Qingshankou is a deep and semi-deep lacustrine facies formation developed in the depressional stage of the basin, which is the main source rock and an important shale oil layer in the northern Songliao Basin. During a period of K_2qn_1, the lake level expanded rapidly, covering an area of 87,000 km^2. And the lake was deep, forming organic-rich shales with thicknesses between 60 and 100 m. In the K_2qn_{2-3} stages, the lake level was lowered and the coverage area decreased to 41,000 km^2 . Large deltaic sedimentary phases were developed on the edge of the sag (Liu et al., 2019) .

Across the whole basin, the lithology and facies varied substantially; deep-lacustrine black mudstones, semi-deep lacustrine black mudstones, and shales were found in Wangfu sag, Sanzhao sag, and Gulong sag, respectively; interlayers of shallow lacustrine sandstones with unequal thickness were found on the edge of the sag (Liu et al., 2019). The distribution pattern of the facies belt from the edge of the basin to the depocenter was fluvial facies, delta facies, semi-deep lacustrine facies, underwater distributary channel facies, and deep lacustrine facies (Figure 1).

Source rock samples are taken for correction of pyrolysis parameters (Table 1), calibration of hydrocarbon generation kinetic parameters (Table 2) and calculation of hydrocarbon expulsion efficiency.

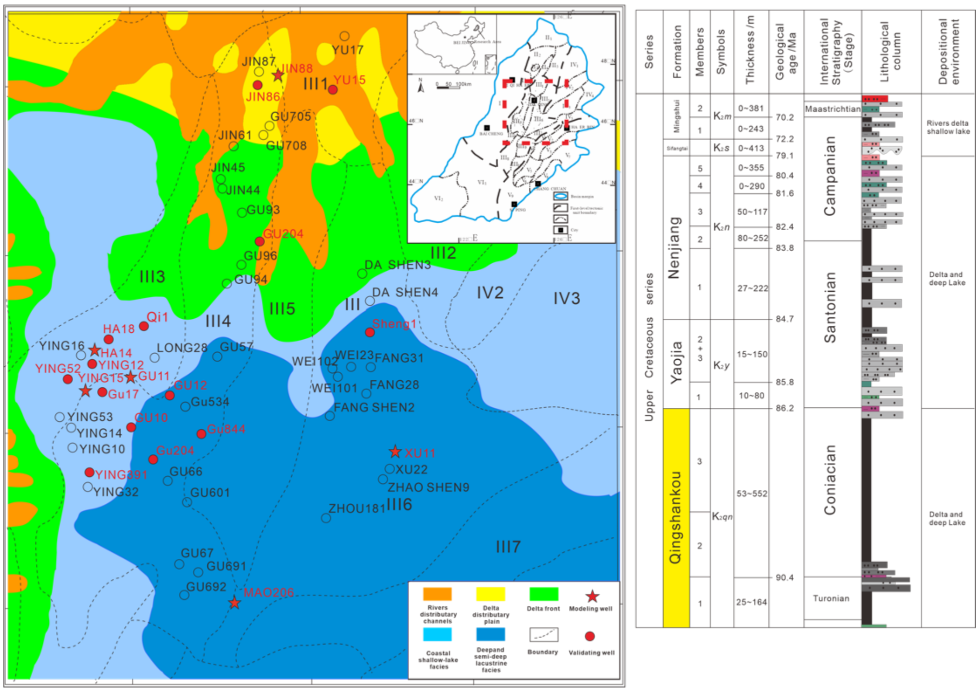

Fig. 1 The sedimentary facies of the Qingshankou Formation (left) and synthetic histogram of the northern Songliao Basin (right). The asterisk symbol well is sampled intensively and was used as a modeling well to calculate HEE for other wells. Red dot symbol wells are sparsely sampled and was used to validate the reliability of the model.

Table 1 Samples for correction of Pyrolysis Parameters

Well number	Depth (m)	TOC (%)	S_1 (mg/g)	S_2 (mg/g)	"A" (%)	HC (mg/g)
Gu10	2464.00	2.36	1.90	3.22	0.44	3.27
Gu10	2464.50	2.04	1.87	3.68	0.55	3.89
Gu10	2465.00	2.63	1.99	3.31	0.48	3.27
Gu10	2466.00	1.97	2.12	3.24	0.53	3.69
Gu10	2472.15	2.61	2.28	3.60	0.57	4.13
Gu11	2431.00	1.96	2.22	4.03	0.63	4.51
Gu11	2433.00	1.98	1.56	3.86	0.54	3.78
Gu12	2371.05	1.66	0.92	1.76	0.24	1.73
Gu12	2372.05	2.13	1.19	2.68	0.33	2.40
Gu12	2373.05	2.47	1.10	2.45	0.29	2.30
Gu17	2365.00	1.91	2.56	6.26	0.58	4.67
Gu17	2366.00	1.86	2.18	4.74	0.79	5.61
Gu17	2367.00	1.61	1.99	4.32	0.69	5.53

Gu17	2368.54	1.39	1.78	4.44	0.61	5.05
Gu17	2369.54	2.02	2.35	5.63	0.77	6.67
Gu204	2376.00	1.47	2.12	5.78	0.58	4.91
Gu204	2380.00	2.84	1.89	11.91	0.57	4.51
Gu204	2384.00	1.54	1.56	6.18	0.55	4.12
Gu204	2388.00	2.31	2.73	10.06	0.84	6.17
Gu204	2392.15	2.92	2.72	14.93	0.96	7.63
Gu844	2579.00	1.60	1.23	1.45	0.23	1.71
Ha14	2050.00	2.89	2.73	11.80	0.85	6.96
Ha14	2054.30	1.08	1.93	4.71	0.60	4.94
Ha14	2060.00	1.70	1.54	6.95	0.64	5.79
Q1	1929.00	1.85	1.06	8.43	0.48	3.02
Q1	1949.00	2.68	1.39	11.49	0.47	2.86
Q1	1991.90	1.13	2.24	4.22	0.44	4.10
Q1	2007.50	2.03	1.67	7.45	0.47	4.09
Q1	2023.50	1.87	1.67	6.98	0.58	5.21
Q1	2046.10	2.43	1.39	10.03	0.44	3.80
Q1	2076.80	2.97	1.19	9.83	0.29	2.57
Q1	2100.30	2.54	1.48	7.25	0.30	2.70
Ying52	2187.30	1.56	2.94	6.27	0.78	6.11
Ying52	2189.00	3.76	2.98	14.32	0.92	7.09
Ying52	2190.35	2.67	2.50	10.76	0.77	5.75
Ying52	2190.60	1.46	1.15	5.27	0.37	2.64

2.2 Error Analysis of Pyrolysis Parameters

Since Tissot et al. (Tissot and Welte, 2013) proposed the theory of "late generation of hydrocarbons from the thermal decomposition of kerogen", researchers have tried to establish an effective experimental method to evaluate the amount of hydrocarbons generated from kerogen. Consequently, the rock pyrolysis technique was developed. The most effective and widely used method of petroleum bearing rock pyrolysis has been applied to Rock-Eval II (Espitalié et al., 1985) and VI (Lafargue et al., 1998) pyrolysis analyzers developed by the French Petroleum Institute (i.e., source rock evaluation system). After the crushed rock samples are pyrolyzed in the instrument, the parameters—free S_1 hydrocarbons (hydrocarbons that are thermally evaporated at temperatures less than 300 °C during the heating process), S_2 hydrocarbons released from pyrolysis (hydrocarbons detected when the rock samples are heated by a temperature program ranging from 300°C to 600°C (or 850°C)), and T_{max} (*pyrolysis temperature* at which the *maximum* amount of hydrocarbon is generated)—are obtained.

The organic matter in the source rock contains extractable residual oil and non-extractable kerogen, and the residual oil is composed of hydrocarbons and non-hydrocarbon compounds (Figure 2). S_1 usually includes low-carbon saturated and aromatic hydrocarbons. Conversely, S_2 contains three components: high-carbon hydrocarbons, hydrocarbons produced from the pyrolysis of *resins and asphaltenes*, and hydrocarbons released from the pyrolysis of kerogen (Banerjee et al., 1998; Copard et al., 2002; Jin and Sonnenberg, 2013; Langford and Blanc-Valleron, 1990; Lehne and Dieckmann, 2007; Rahman et al., 2000). Generally, S_1 and S_2 are regarded as residual hydrocarbons and residual hydrocarbon generation potential. However, due to the experimental procedure of rock pyrolysis, some heavy hydrocarbons with a boiling point higher than 300 °C and some hydrocarbons produced from *the thermal decomposition of resins and asphaltenes* enter the hydrocarbons released from cracking (these two components are commonly denoted as ΔS_2 in source rock analysis). Therefore, the residual hydrocarbon amount (S_1) is underestimated, and the hydrocarbon-generation potential of kerogen (S_2) is overestimated, so that the hydrocarbon expulsion efficiency calculated from the pyrolysis parameters before correction is higher than the actual value.

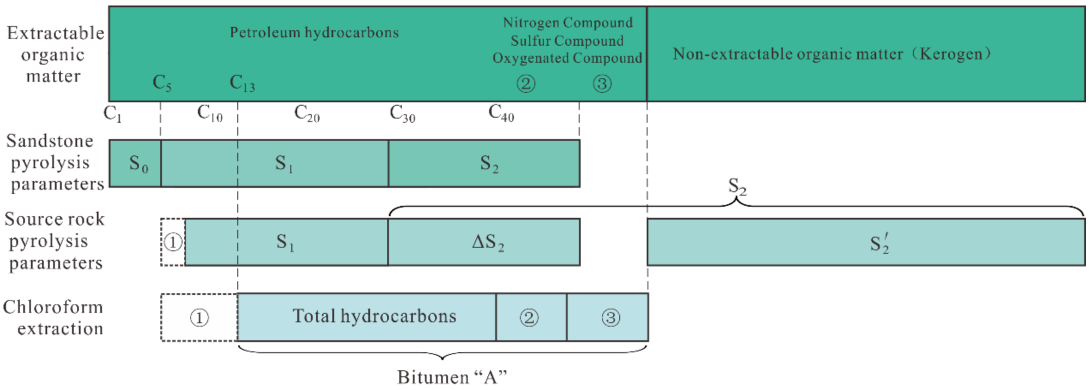

Comment: ①. Light hydrocarbon loss ②. Non-hydrocarbon ③. Asphaltene

Fig. 2 Distribution of pyrolysis parameters in hydrocarbon components(The figure is taken from (Bordenave, 1993))

2.3 Correction of pyrolysis parameters

In this paper, an improved experimental method was adopted to correct this effect(Figure 3). *Sample Treatment.* Samples from different burial depths were selected(Table 1), crushed, and mixed evenly. The sample was divided into two parts, and one part was directly pyrolyzed to determine S_2. For the other part, chloroform extraction was performed first followed by pyrolysis to determine S_2'. Then, the source rock's residual hydrocarbon is S_1' (see formula 1-2), and the residual hydrocarbon generation potential of the source rock is S_2'.

$$S_1'=S_1+\Delta S_2 \quad (1)$$

$$\Delta S_2=S_2-S_2' \quad (2)$$

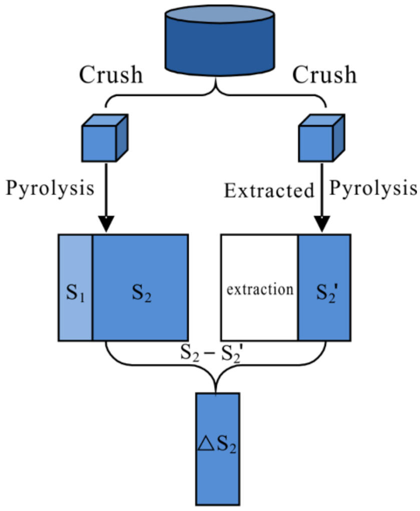

Fig. 3 Experimental scheme for the correction of pyrolysis parameters

The correction coefficient is the ratio of the pyrolysis parameters after correction to that before correction. The results show significant differences before and after correction of S_1 and S_2 (Figure 4); the overall correction coefficients of S_1 and S_2 are 3.04 and 0.41, respectively. The correction coefficient of the pyrolysis parameter S_2 is related to the maturity of the sample itself, samples with high maturity (T_{max}>445°C) is lower than that with low maturity (T_{max}<445°C), respectively 0.53 and 0.25.

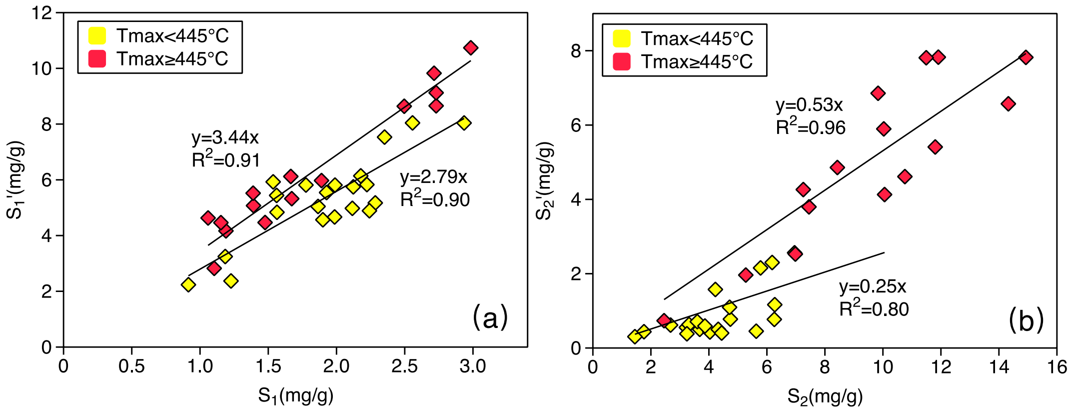

Fig. 4 Analysis of 38 samples showing the correlation diagram of Pyrolysis parameters

before and after extraction (a: S_1; b: S_2)

2.4 Calculation of hydrocarbon expulsion efficiency (K)

The schematic diagram for calculating the hydrocarbon expulsion efficiency based on the principle of mass balance method is as follows (Figure 5). In the original state, the hydrocarbon generation potential of the source rock is S_2^o. As the depth of the formation increases, kerogen begins to generate hydrocarbons, and part of the hydrocarbon generation potential is converted into hydrocarbon generation Q_g, the residual hydrocarbon generation potential is S_2'. When hydrocarbon generation accumulates to a certain extent, the source rock begins the process of hydrocarbon expulsion, the amount of hydrocarbon expulsion is Q_e, and the residual hydrocarbon is S_1'. The principle of conservation of hydrocarbon generation and expulsion can be expressed as: at any time, the sum of the source rock's hydrocarbon generation (Q_g) and the residual hydrocarbon generation potential (S_1') is the original hydrocarbon generation potential (S_2^o), and the sum of the hydrocarbon expulsion (Q_e) and residual hydrocarbon (S_1') is hydrocarbon generation (Q_e).

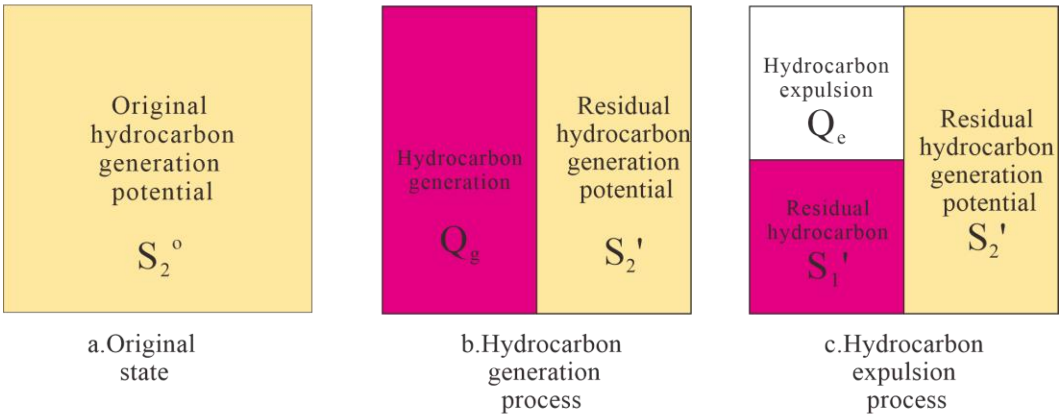

Fig. 5 Mass balance of source rocks in the process of hydrocarbon generation and expulsion（a: original state; b: Hydrocarbon generation process； c: Hydrocarbon expulsion process. ）

The formula for calculating the hydrocarbon expulsion efficiency K can be written as (Equation 3-5):

$$K = \frac{Q_e}{Q_g} \tag{3}$$

$$Q_g = S_2^o - S_2' \tag{4}$$

$$Q_e = S_2^o - S_1' - S_2' \tag{5}$$

S_1' and S_2' can be obtained from the pyrolysis parameter correction experiment, , S_2^o need be recovered by S_2' and hydrocarbon generation conversion rate F (Wang et al., 2011), according to the principle of hydrocarbon generation kinetics (Equation 6) .

$$S_2^o = \frac{S_2'}{1-F} \tag{6}$$

The black mudstone samples of different kerogen types (I, II_1, II_2, III) from the Qingshankou Formation were subjected to hydrocarbon thermal simulation experiments in the study area to determine the hydrocarbon generation conversion rate

F (Table 2).

Table 2 Samples for calibration of hydrocarbon generation kinetic parameters

Kerogen type	I	II_1	II_2	III
Well number	Sheng1	Gu601	Long28	Gu94
R_o	0.41	0.7	1.19	0.52
TOC (%)	3.77	1.36	0.26	1.38
T_{max} (℃)	440	440	451	438
S_1 (mg/g)	1.07	0.64	0.11	0.22
S_2 (mg/g)	11.15	12.53	2.10	0.24
HI (mg/g)	1139	920	794	384

In the experiment, Rock-Eval-II pyrolysis apparatus was used, and the samples were heated from 200°C to 600°C at a heating rate of 10°C/min, 20°C/min, and 40°C/min. The relationship between the amount of product and the heating time was recorded in real time. The curve describing the relationship of the conversion rate of oil generation and the gas generation with temperature was obtained. It was used to calibrate the hydrocarbon-generation kinetic parameters (Wang et al., 2011); A parallel first-order reaction chemical kinetics model was used to perform the fitting, and the chemical kinetic parameters of hydrocarbons generated from the organic matter were obtained (Table 3 and Table S1-S3).

Table 3 Kinetic parameters of the gas and oil reaction of organic matter in the Sheng1 well sample

Gas Activation Energy (kJ/mol)	Pre-exponential factor (min)	Original reactive potential	Oil Activation Energy (kJ/mol)	Pre-exponential factor (min)	Original reactive potential
160	7.472×10^{15}	4.497×10^{-4}	140	3584.438	5.356×10^{-7}
170	4.995×10^{10}	7.850×10^{-9}	150	1.762×10^{13}	3.426×10^{-3}
180	3.269×10^{12}	9.219×10^{-7}	160	1.570×10^{17}	3.380×10^{-4}
190	9.170×10^{9}	1.443×10^{-7}	170	3.971×10^{12}	3.415×10^{-7}
200	1.819×10^{-2}	3.187×10-10	180	1.143×10^{17}	4.507×10^{-3}
210	5.125×10^{18}	5.480×10^{-3}	190	1.510×10^{14}	0.992
220	4.498×10^{15}	4.398×10^{-2}	200	1205131	9.228×10^{-8}

230	4.096×10^{9}	2.562×10^{-8}	210	2.110×10^{11}	1.205×10^{-7}
240	1.456×10^{18}	0.884	220	5.362×10^{11}	3.854×10^{-7}
250	1.197×10^{20}	5.772×10^{-2}	230	8.764×10^{11}	2.838×10^{-7}
260	9.093×10^{15}	6.803×10^{-7}	240	9.718×10^{11}	1.436×10^{-8}
270	6.912×10^{16}	7.270×10^{-3}	250	9.957×10^{11}	4.452×10^{-7}
280	1.644×10^{14}	6.965×10^{-4}	260	9.981×10^{11}	2.117×10^{-7}
290	1.130×10^{14}	5.632×10^{-4}	270	1.001×10^{12}	4.764×10^{-7}
300	1.026×10^{14}	2.013×10^{-5}	280	1.002×10^{12}	4.571×10^{-7}
310	1.004×10^{14}	1.193×10^{-4}	290	1.001×10^{12}	3.332×10^{-8}
320	1.003×10^{14}	1.900×10^{-9}	300	1.001×10^{12}	2.003×10^{-7}
330	1.001×10^{14}	9.579×10^{-10}	310	1.001×10^{12}	2.305×10^{-7}
340	1.000×10^{14}	1.070×10^{-9}	320	1.000×10^{12}	1.866×10^{-7}
Average activation energy: 239.900kJ/mol			Average activation energy: 189.902kJ/mol		

As shown in Figure 6, using the above model, the calculated conversion rate of the hydrocarbons generated from organic matter under the experimental conditions exhibited an excellent fit to the experimental points, demonstrating the feasibility of the selected model as the basis for the next geological application.

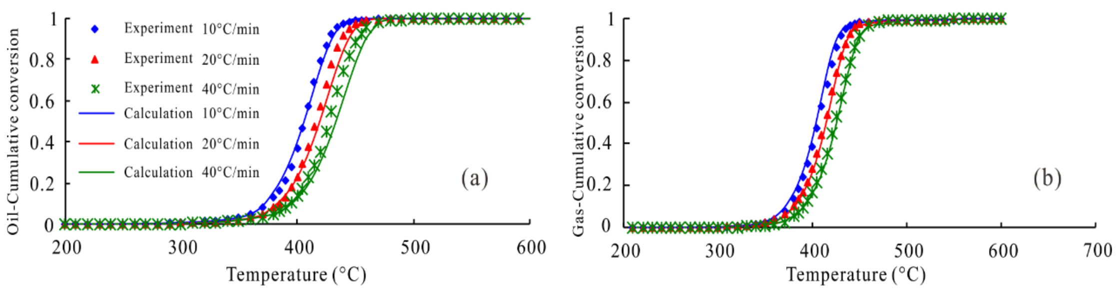

Fig. 6 Conversion rate curves of hydrocarbons generated from organic matter in mudstone from the Sheng 1 well (a: oil generation; b: gas generation)

The geological application of the kinetic model of hydrocarbon generation from organic matter needs to be combined with the kerogen type, the depositional and burial history (Wang et al., 2011). The kerogen type data for this study area were obtained from the Daqing Oilfield Geochemical Database. The depositional and burial history and the thermal history used in this study were derived from a combination of the eroded strata thickness of the Songliao basin since the Mesozoic era and the present stratigraphic data. Based on this, the hydrocarbon-generation potential of the source rock of the Qingshankou of wells could be recovered (Figure S1). Figure 7 depicts the hydrocarbon-generation conversion rate profile of the hydrocarbon source rock from the of the Ha-14 well, and the profile was obtained from a combination of the calibrated hydrocarbon-generation kinetics model of organic matter, the kerogen type, the depositional and burial history and the thermal history data of a single well in each study area for geological application purposes.

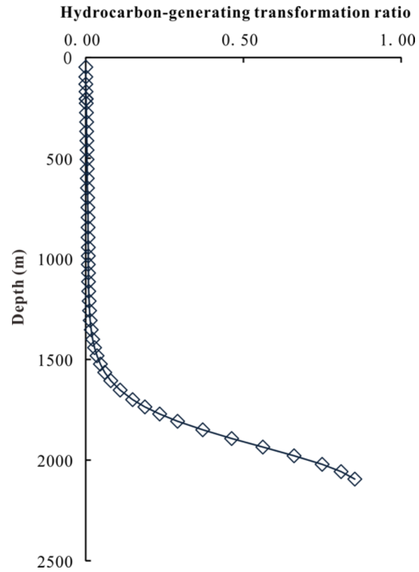

Fig. 7 Conversion rate profile of the hydrocarbon generation of the Ha-14 well

2.5 Evaluation of source rocks using well logging analysis

In the study of hydrocarbon expulsion efficiency, due to the limitation of sample source and the funds for analysis, the analytical data available to a laboratory are limited. It is challenging to meet the needs of fair evaluation and exploration, thus leading to inaccurate results. However, the logging curve has played an essential role in more and more studies since continuity is its advantage, and the organic heterogeneity has a corresponding excellent relationship with the logging curve. In this study, the improved

△ logR technique (Kamali and Mirshady, 2004) was used for modeling with geochemical parameters, including S_1' and S_2' of the modeling well (Table S4). An excellent correlation was found between the measured (Table 4) and calculated values of Ha14 (modeling well); the comprehensive effect is shown in Figure 8.

Table 4 Geochemical parameters of Ha 14 sample

Sample number	Depth (m)	S1' (mg/g)	S2' (mg/g)	"A" (%)	HC (%)
1	1952.7	1.69	1.81	0.14	1.15
2	1957.7	2.04	1.63	0.14	1.55
3	1963.7	2.57	1.77	0.26	2.04
4	1967.7	2.95	2.78	0.28	2.12
5	1971.9	2.96	3.31	0.27	1.96
6	1975.4	2.76	2.18	0.26	2.10
7	1982.4	3.65	1.85	0.46	3.10
8	1987.4	5.43	1.65	0.68	4.93
9	1991.9	3.99	1.61	0.51	3.51
10	2005.9	7.79	1.22	0.99	7.43
11	2014	5.12	1.49	0.58	4.67
12	2025	5.87	1.75	0.70	5.34
13	2029.7	5.43	1.06	0.64	5.11
14	2033.5	4.20	1.37	0.87	3.80
15	2035.4	3.43	0.99	0.62	3.14
16	2038	2.74	1.66	0.31	2.24
17	2041	4.88	3.41	0.47	3.85
18	2045.2	5.77	3.30	0.60	4.78
19	2048.15	6.76	8.49	0.19	4.21
20	2049.1	5.17	3.81	0.54	4.03
21	2053.2	4.96	1.35	0.56	4.56
22	2055.7	4.69	5.13	0.38	3.15
23	2059.3	5.05	2.91	0.50	4.17
24	2062.3	5.14	5.87	0.40	3.38
25	2068.3	4.84	4.88	0.56	3.38
26	2073.8	4.57	3.96	0.40	3.38
27	2076.3	8.29	11.01	0.37	4.98
28	2077.5	7.69	6.44	0.33	5.75
29	2080.3	8.02	6.11	0.67	6.19

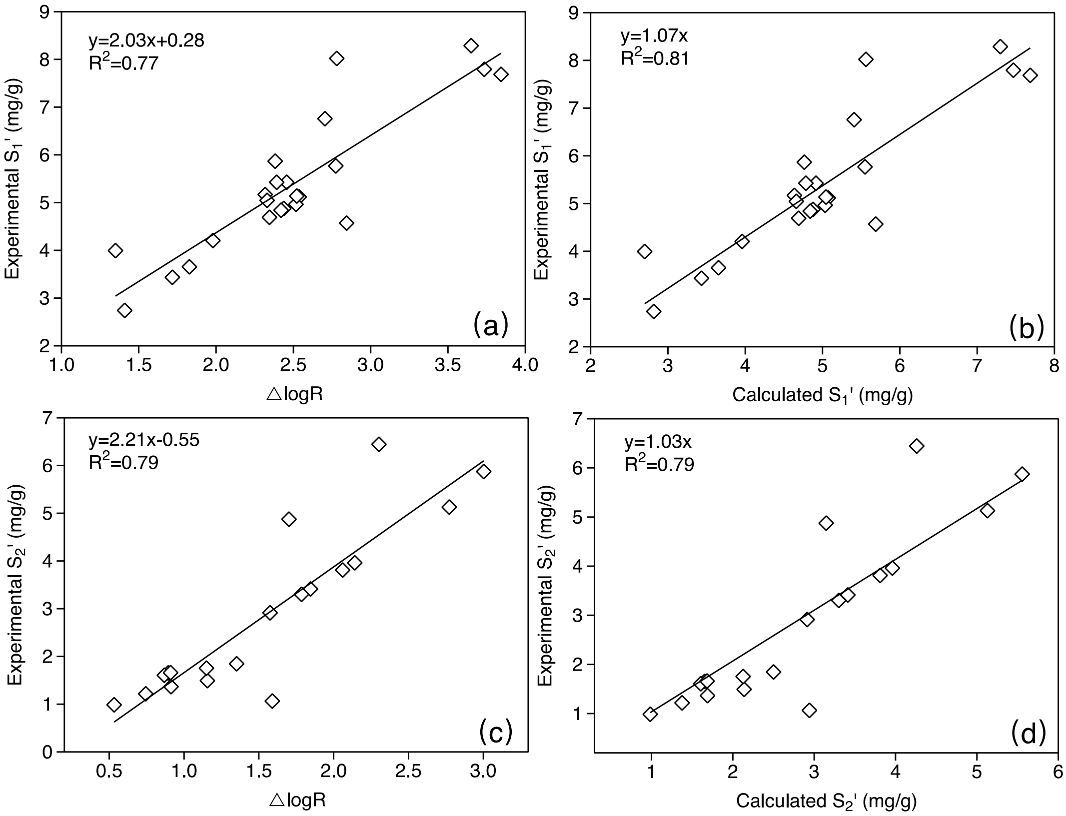

Fig. 8 Correlation of measured S_1' and S_2' of the Ha-14 well between the modeled and calculated values. The applicability effect of other modeling wells can be seen in Figure S2-S5.

The calculation process of the application well hydrocarbon expulsion efficiency is as follows: first, the ΔlogR model is used to calculate S_1' and S_2' for non-modeling wells, then S_2' is combined with the hydrocarbon generation conversion rate profile F to calculate S_2^o, and finally, the hydrocarbon expulsion efficiency is calculated according to formula (3-6).

3 RESULTS AND DISCUSSION

3.1 Hydrocarbon expulsion efficiency calculation using corrected pyrolysis parameters

It can be seen from the calculation results of Ha14 in Table 5 and Figure 9 that the average hydrocarbon generation amount, the hydrocarbon expulsion amount, and the hydrocarbon expulsion efficiency calculated using the pyrolysis parameters before correction were 14.5 mg/g, 13.7 mg/g, and 94.2%, respectively. The corresponding values using the corrected pyrolysis parameters were 12.9 mg/g, 9.9 mg/g, and 76.7%. It can be seen that it is necessary to use the corrected pyrolysis parameters to calculate the hydrocarbon expulsion efficiency.

Table 5 Calculation results of hydrocarbon expulsion efficiency before and after correction of pyrolysis parameters of Well Ha14

Sample type	Q_g (mg/g)	Q_e (mg/g)	K (%)
Before correction	14.5	13.7	94.2
After correction	12.9	9.9	76.7

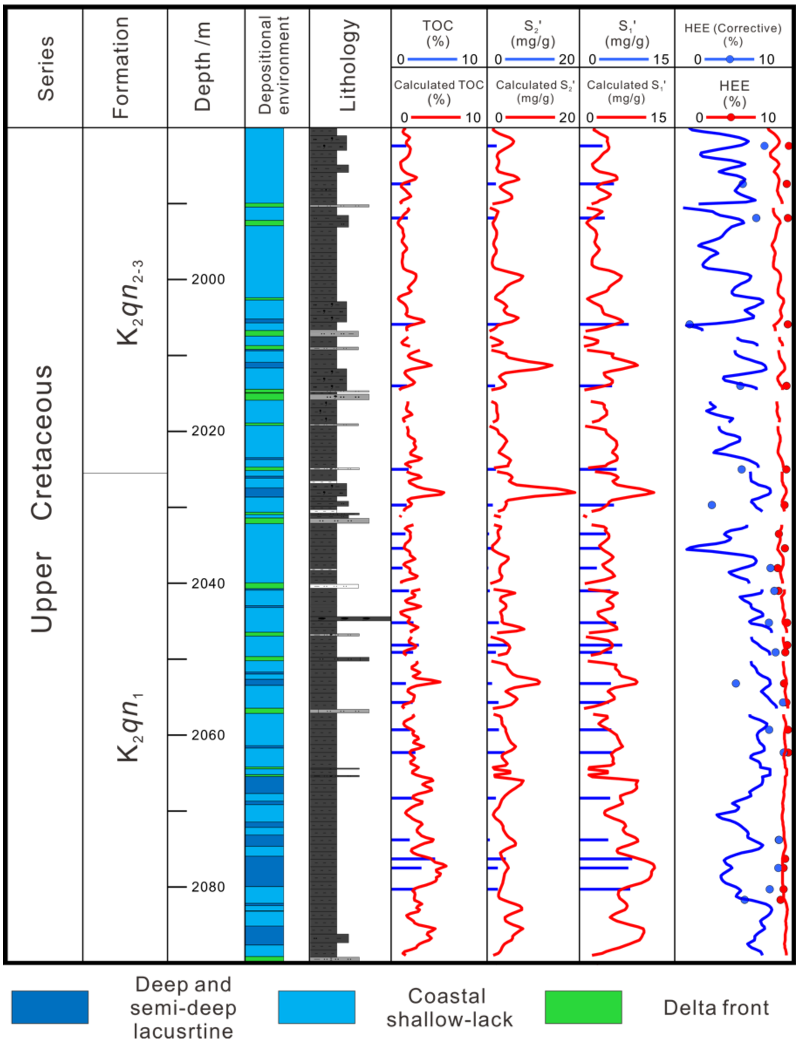

Fig. 9 Profiles of calculated hydrocarbon expulsion efficiency and geochemical parameters of the Ha14 well

3.2 Factors affecting the hydrocarbon expulsion efficiency

The hydrocarbon expulsion efficiency is used to study the efficiency of primary migration, and there are numerous common factors shared by the factors that affect the hydrocarbon expulsion efficiency and those affecting primary migration. Temperature, pressure, stress, fluid potential, compaction and under compaction, pores of sedimentary rocks, porosity and pore structure, absolute permeability, relative permeability, critical migration saturation, specific surface, adsorption and wettability, interfacial tension, capillary pressure and displacement pressure, critical temperature, critical pressure, and diffusion all have a strong influence on the hydrocarbon expulsion efficiency (Singh and Singh, 1994; Singh, 2011).

By summarizing these abovementioned factors, this paper studied the effects of related parameters on the hydrocarbon expulsion efficiency of source rocks from six aspects: (i) abundance of organic matter, (ii) type of organic matter, (iii) maturity of organic matter, (iv) source-reservoir collocation relation, (v) sedimentary facies.

1) Abundance of organic matter

Organic matter abundance refers to the amount of organic matter per unit mass of rock. When other conditions are similar, a higher content (abundance) of organic matter in the rock indicates a higher hydrocarbon generation capacity and higher hydrocarbon expulsion efficiency. The abundance of organic matter is usually expressed as total organic carbon (TOC, %). As can be seen from the scatter plots of TOC and the hydrocarbon expulsion efficiency for the Ha 18 well, Ying 12 well, Mao 206 well and Xu 11 well, when TOC was less than 2–3%, the hydrocarbon expulsion efficiency increased with increasing TOC; when TOC was higher than 2–3%, the change was not that significant (as shown in Figure 10). Mineral and organic pore surfaces have a retention effect on hydrocarbons. When TOC exceeds a certain threshold (2-3% in this study), the retention capacity of minerals for hydrocarbons is saturated. In this case, as TOC increases, the amount of hydrocarbon generation from organic matter increases in proportion to the amount of retained hydrocarbons, which results in no significant change in hydrocarbon expulsion efficiency.

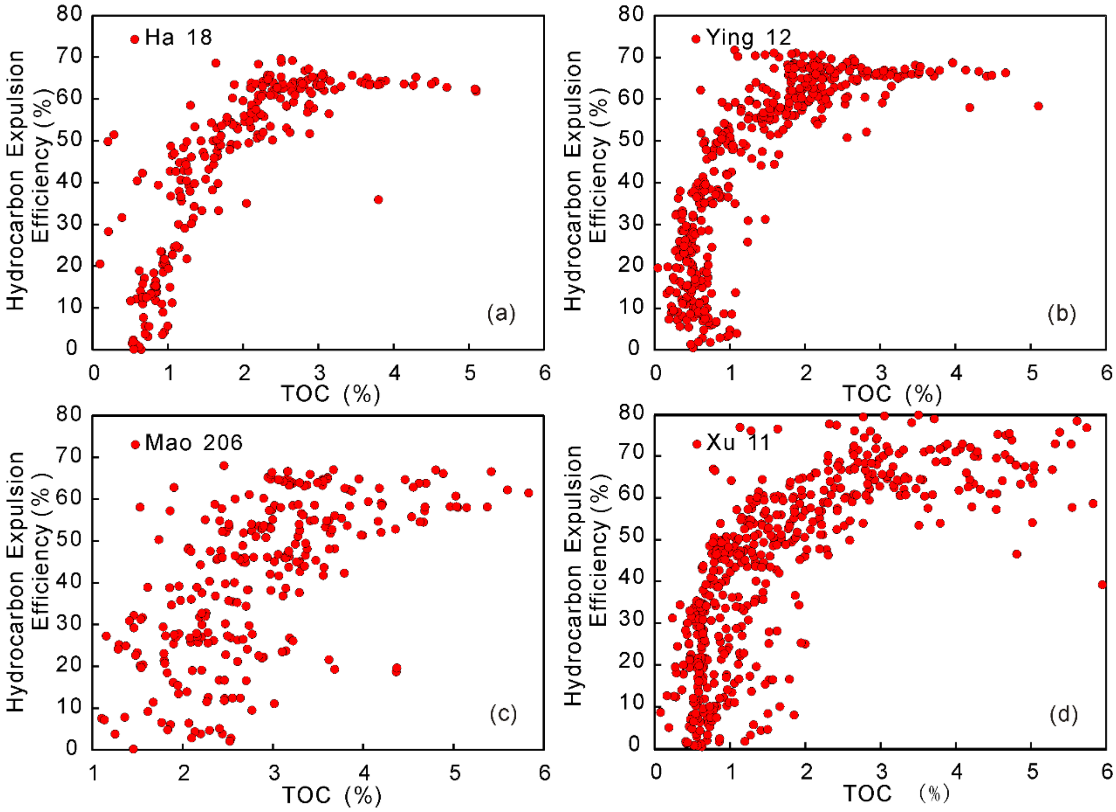

Fig. 10 Scatter plot of the hydrocarbon expulsion efficiency（The TOC of the four wells Ha18, Ying12, Mao206, and Xu11 vary significantly along the vertical direction, suitable for studying the influence of organic matter abundance on the efficiency of hydrocarbon expulsion.)

2) Type of organic matter

SY/T 5125-1996 method (Li et al., 2016; Pan et al., 2015; Shi et al., 2018) was used to determine maceral group composition of kerogen and its classification in transmitted light and fluorescent light microscopy. According to TI index (Equation 7), the kerogen is divided into Type I (oil-type, 80< TI< 100), Type II_1 (oil-type, 40< TI< 80), Type II_2 (gas-type, 0< TI <40), and Type III (gas-type, TI< 0). a, b, c, d represent the percentage of the sapropelinite, exinite, vitrnite, intertinite.

$$\mathrm{TI} = \frac{a\cdot(+100)+b\cdot(+50)+c\cdot(-75)+d\cdot(-100)}{100} \quad (7)$$

As shown in Figure 11, the Ying 16 well and Yu 15 well exhibited a corresponding excellent relationship between the hydrocarbon expulsion efficiency and the type of organic matter. With a similar degree of maturity, the better the type of organic matter, the higher the hydrocarbon expulsion efficiency (Type Ⅰ > Type Ⅱ$_1$> Type Ⅱ$_2$ > Type Ⅲ).

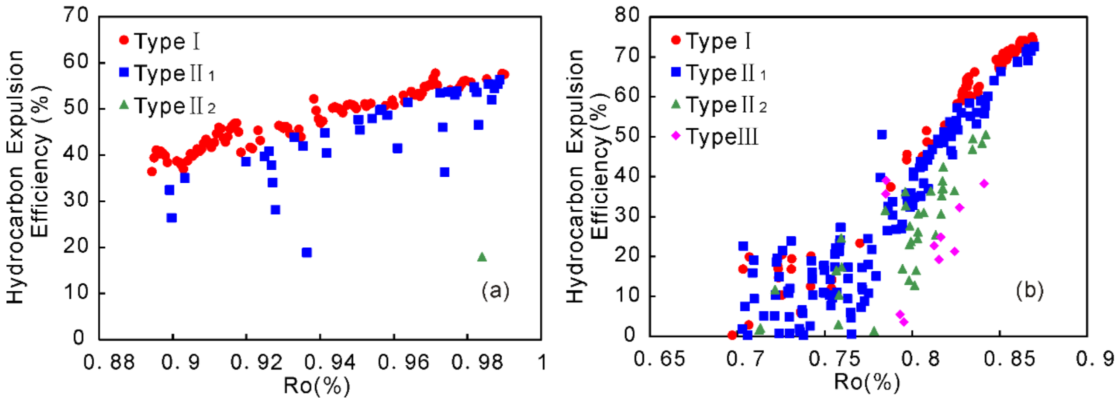

Fig. 11 Relationship between R_o and the hydrocarbon expulsion efficiency (The organic matter maturity and rock types of Ying16 and Yu15 wells vary significantly in the vertical direction, and it is easy to analyze the controlling factors of hydrocarbon expulsion efficiency.)

3) Maturity of organic matter

Figure 12 shows the scatter plots of the organic matter maturity and hydrocarbon expulsion efficiency for the Ying 16 well and Yu 15 well. It can be seen from the figure that the hydrocarbon expulsion efficiency increased with increasing maturity. The factors affecting the hydrocarbon expulsion efficiency, including the abundance and type of organic matter that might exist in the adjacent points, but overall, the higher the maturity, the higher the hydrocarbon expulsion efficiency.

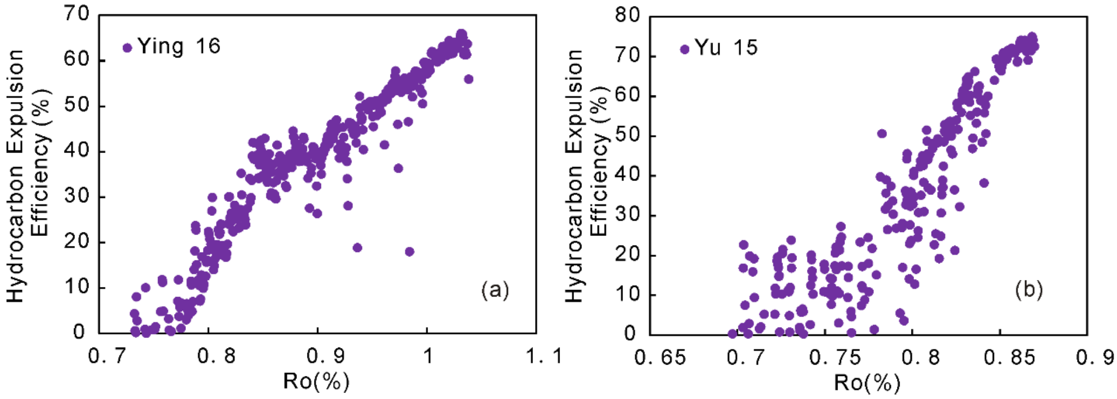

Fig. 12 Scatter plot showing the relationship between organic matter maturity and the hydrocarbon expulsion efficiency for the Ying 16 well and Yu 15 well

4) Source-reservoir co-location relationship

The source-reservoir co-location relationship refers to the combination pattern of source rocks and the sandstones distributed in the source rocks. The hydrocarbon expulsion of source rocks depends on the fact that a thinner single layer of mudstone results in more intercalations of sandstone and mudstone and a higher hydrocarbon expulsion efficiency. According to statistical analysis, four main types of source-reservoir co-location relationships of the source rocks from the Qingshankou Formation in Songliao Basin exist (Table 6).

Table 6. Source-reservoir co-location relationships of source rocks

Source-reservoir co-location relationship	Feature description	Quantitative description
Thick mudstones	Large sets of pure mudstones without sandstones	$L_m \geq 5$m
Thin sandstone interbedded in thick mudstones	Thin sandstone intercalated into mudstones	$L_m<5$m, $L_m/(L_m+L_{s1}+L_{s2})>60\%$
Sandstone-mudstone interlayers	Interlayered thin sandstones and thin mudstones	$L_m<5$, $40\% \leq L_m/(L_m+L_{s1}+L_{s2}) \leq 60\%$

Thin mudstone interbedded in thick sandstones	Thin mudstone intercalated into sandstones	$L_m<5$, $L_m/(L_m+L_{s1}+L_{s2})<40\%$

Note: L_m—thickness of a single layer of mudstone, m; L_{s1}—upper sandstone in contact with mudstones, m; L_{s2}—lower sandstone in contact with mudstones, m;

Four cores with different source-reservoir collocation relationships were sampled intensely, corresponding geochemical analyses were carried out to determine the hydrocarbon expulsion efficiency, and the effects of different source-reservoir collocation relationships on the hydrocarbon expulsion efficiency were analyzed (see Figure 13).

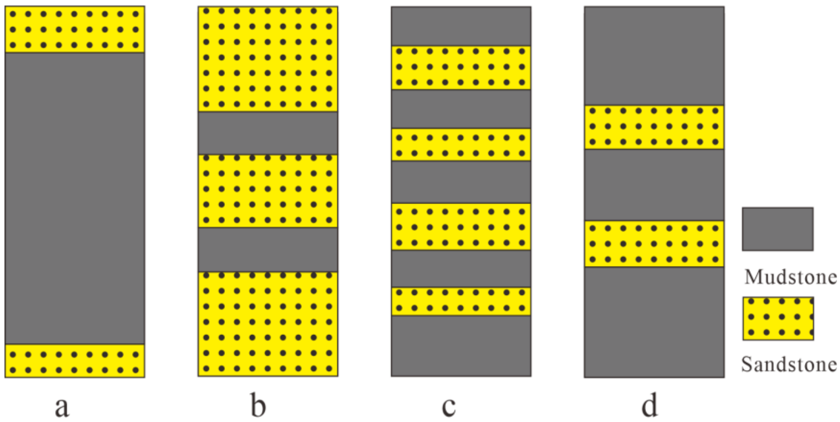

Fig. 13 Sampling design diagram for the source-reservoir collocation relationship

a: Thick mudstone; b: Thin sandstone interbedded in thick mudstones; c: Sandstone-mudstone interlayer; d: Thin mudstone interbedded in thick sandstones

Jin86 well has a complicated source-storage configuration relationship, as shown from the single well profile (Figure 14); the hydrocarbon expulsion efficiency in the middle of the thick mudstone was lower than that of the mudstone adjacent to the sandstone at the interface. The average hydrocarbon expulsion efficiencies of the 18-meter and 8-meter-thick mudstones were 53% and 62%, respectively, and the greater the thickness of the mudstone, the lower is the hydrocarbon expulsion efficiency. The hydrocarbon expulsion efficiencies of two members of thin mudstone interbedded in thick sandstones between 1945 and 1950 meters were 67.1% and 71.5%, respectively. It can be seen from the Jin86 well that the hydrocarbon expulsion efficiencies were ranked as thin mudstone interbedded in thick sandstones > thick mudstones. Figure 15 shows the relationship between organic matter abundance and hydrocarbon expulsion efficiency in the mudstones with different source-reservoir collocation relationships. It can be seen from the figure that the pattern of the hydrocarbon expulsion efficiencies for different collocation relationships was as follows: thin mudstone interbedded in thick sandstones > sandstone-mudstone interlayer > thin sandstone interbedded in thick mudstones > thick mudstones.

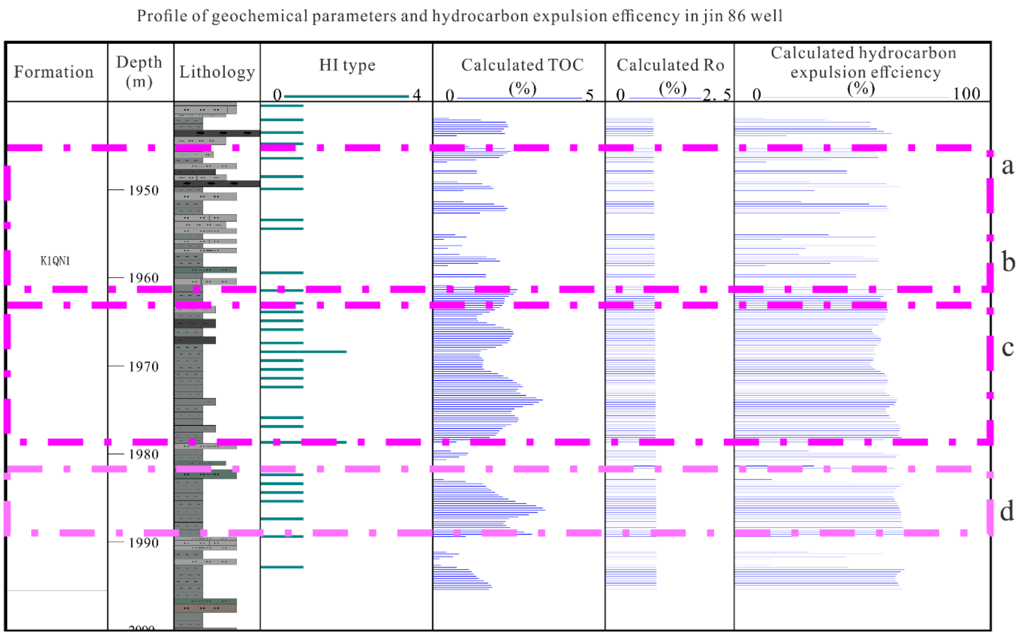

Fig. 14 Profile of the geochemical parameters and hydrocarbon expulsion efficiency (corrected) of the Jin86 well（a. Thin mudstone interbedded in thick sandstone: 67.1%）（b. Thin mudstone interbedded in thick sandstone: 71.5%） (c. The average hydrocarbon expulsion efficiencies of the 18-meter -thick mudstone was lower than

that of the mudstone adjacent to the sandstone at the edge, was 53%) (d. The average hydrocarbon expulsion efficiencies of the 18-meter -thick mudstone was lower than that of the mudstone adjacent to the sandstone at the edge, was 53%)

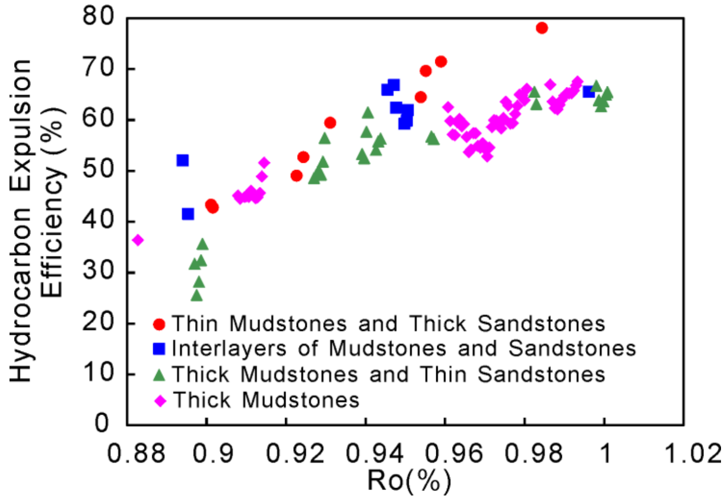

Fig. 15 Relationship between the organic matter maturity of the mudstones with different source-reservoir collocation relationships and the hydrocarbon expulsion efficiency in the strata of the Qingshankou Formation in northern Songliao Basin

5) Sedimentary facies

For different sedimentary facies belts, the type and abundance of organic matter in the mudstone are different, the composition and physical properties of the rock minerals are different, and the source-reservoir collocation relationship is different. Figure 16 shows the sedimentary facies of the Qingshankou Formation of the northern Songliao Basin. As can be seen, the Qingshankou Formation was mainly divided into five sedimentary facies: underwater distributary channel, delta front, delta distributary plain, coastal shallow lacustrine facies, and deep-lacustrine and semi-deep lacustrine facies.

For different sedimentary facies, Figure 16 shows the relationship between the mean predicted hydrocarbon expulsion efficiency of wells in a small range of R_o and the corresponding R_o. It can be seen that the hydrocarbon expulsion efficiencies of different sedimentary facies within the same maturity range were ranked as follows: underwater distributary channel > delta distributary plain > delta front > deep lacustrine and semi-deep lacustrine facies. The higher the sand content in sedimentary facies, the better the pore permeability of inorganic minerals and the higher the hydrocarbon expulsion efficiency.

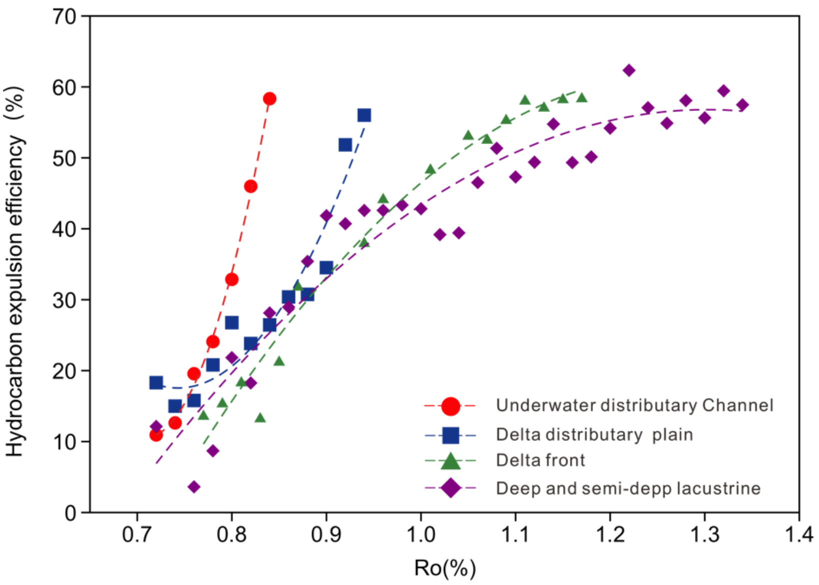

Fig. 16 Relationship between Ro and the average corresponding hydrocarbon expulsion efficiency（The underwater channel facies samples are from Well Yu15, the semi-deep lake facies samples are from Well Xu11, and the delta plain facies samples are from Well Jin86.)

Note that the HEE is intrinsically determined by both the residual hydrocarbon amount (light hydrocarbon fraction, heavy hydrocarbon fraction) and the S2o (original hydrocarbon generation potential). In this work, the crude oil of the Qingshankou is characterized by generally high density and low proportion of light hydrocarbons in the residual hydrocarbons, so only the correction method for heavy hydrocarbons is focused on. In fact, for lighter oils, non-confined coring and long core placement can cause significant light hydrocarbon losses, which can bias the calculation of hydrocarbon removal efficiency. Future work will focus on the correction of light hydrocarbon losses.

4 CONCLUSIONS

In the present investigation, the corrected pyrolysis parameters were used to calculate the hydrocarbon expulsion efficiency of mudstone and to understand the evaluation of hydrocarbon expulsion efficiency more accurate. The following conclusions are drawn:

(1) The average hydrocarbon expulsion efficiencies of the Ha14 well before and after correction of the pyrolysis parameters were 94.2% and 76.7%, respectively, with a difference of 17.5%.

(2) The effects of the abundance, type, and maturity of organic matters on the amount of generated hydrocarbons and the residual hydrocarbon amount were analyzed concerning the calculation of the hydrocarbon expulsion efficiency. The results showed that: (a.) when TOC $<$ 2–3%, the hydrocarbon expulsion efficiency increased with increasing organic matter abundance; when TOC $>$ 2–3%, the change was not substantial; (b.) The oil-type organic matter has a higher hydrocarbon-expulsion efficiency than the gas-type organic matter; (c.) The higher the maturity of organic matter, the higher the hydrocarbon expulsion efficiency.

(3) The impact of the source-reservoir collocation relationship on the hydrocarbon expulsion efficiency was analyzed. In terms of the average hydrocarbon expulsion efficiency, the values were ranked as thin mudstone interbedded in thick sandstones $>$

sandstone-mudstone interlayer> thin sandstone interlayer in thick mudstones > thick mudstones; the closer the thick mudstone to the interface, the higher the hydrocarbon expulsion efficiency.

(4) The impact of sedimentary facies on the hydrocarbon expulsion efficiency was analyzed, and the hydrocarbon expulsion efficiencies were ranked as underwater distributary channel > delta distributary plain > delta front> deep lacustrine and semi-deep lacustrine facies.

A clear understanding of source rock analysis assumptions is needed for improved evaluation of unconventional oil and gas resources. The more accurate the hydrocarbon expulsion efficiency is, the better evaluated results of both conventional and unconventional petroleum resources will be. We will continue working on the impact factors of hydrocarbon expulsion efficiency in the future.

ACKNOWLEDGEMENTS

This study was partly funded by the National Natural Science Foundation of China (42072160, 41922015), National Science and Technology Major Project (2016ZX05004-001, 2016ZX05007-003).

DECLARATIONS

Conflict of interest: We declare that we have no financial or personal relationships *with other people or organizations that can inappropriately influence our work, there is no professional or other personal interest of any nature or kind in any product, service and/or company that could be construed as influencing the position presented in, or the review of, the manuscript entitled, "Calculation and affecting factors of hydrocarbon expulsion efficiency using corrected pyrolysis parameters".*

Ethical approval: Not required

AUTHOR CONTRIBUTIONS

Haitao Xue designed the project and wrote the main manuscript. Shansi Tian help to draw the figures and to draft the manuscript. Shuangfang Lu and Min Wang defined the statement of problem. Hugh Christopher Greenwell help to discuss the problems and revise the manuscript. Peng Luo and Zhentao Dong help to discuss the main idea and help to draft the manuscript. Wenhua Zhang and Shudong Lu help to calculate the data and draw the figures. Ma Wei and Yifeng Wang help to revise the figures. All authors reviewed the manuscript.

REFERENCES

Banerjeea, A., Sinha, A.K., Jain, A.K., Thomas, N.J., Misra, K.N., Chandra, K., 1998. A mathematical representation of Rock-Eval hydrogen index vs Tmax profiles. Organic geochemistry, 28(1-2), 43-55. https://doi.org/10.1016/S0146-6380(97)00119-8

Behar, F., Kressmann, S., Rudkiewicz, J.L. and Vandenbroucke, M., 1992. Experimental simulation in a confined system and kinetic modelling of kerogen and oil cracking. Organic Geochemistry, 19(1-3), 173-189. https://doi.org/10.1016/0146-6380(92)90035-V

Behar, F., Vandenbroucke, M., Teermann, S.C., Hatcher, P.G., Leblond, C., Lerat, O.,1995. Experimental simulation of gas generation from coals and a marine kerogen. Chemical Geology, 126(3-4), 247-260. DOI：10.1016/0009-2541(95)00121-2

Blanc, P. and Connan, J., 1992. Generation and expulsion of hydrocarbons from a Paris Basin Toarcian source rock: An experimental study by confined-system pyrolysis. Energy & fuels, 6(5), 666-677. DOI:10.1021/ef00035a020

Liu, B., Bechtel, A., Sachsenhofer, R.F., Gross, D., Gratzer, Reinhard, Chen, Xuan, 2017. Depositional environment of oil shale within the second member of Permian Lucaogou Formation in the Santanghu Basin, Northwest China. International Journal of Coal Geology, 175, 10-25. https://doi.org/10.1016/j.coal.2017.03.011

Bordenave, M.L., 1993. Applied petroleum geochemistry, Frist ed. Technip, Paris.

Chen, R., Wang, H., Chen, J. and Liu, Y., 2015. An Experimental Method to Evaluate the Hydrocarbon Generation and Expulsion Efficiency in the Songliao Basin. Natural Gas Geoscience, 26(5), 915-921. DOI: 10.11764/j.issn.1672-1926.2015.05.0915

Copard, Y., Disnar, J.R. and Becq-Giraudon, J.F., 2002. Erroneous maturity assessment given by Tmax and HI Rock-Eval parameters on highly mature weathered coals. International Journal of Coal Geology, 49(1), 57-65. https://doi.org/10.1016/S0166-5162(01)00065-9

Dembicki Jr, H., Horsfield, B. and Ho, T.T., 1983. Source rock evaluation by pyrolysis-gas chromatography. AAPG Bulletin, 67(7), 1094-1103. https://doi.org/10.1306/03B5B709-16D1-11D7-8645000102C1865D

Dickey, P.A., 1975. Possible primary migration of oil from source rock in oil phase: Geologic notes. AAPG bulletin, 59(2), 337-345. DOI：10.1306/83d91c8b-16c7-11d7-8645000102c1865d

Espitalié, J., Deroo, G. and Marquis, F., 1985. La pyrolyse Rock-Eval et ses applications. Deuxième partie. Revue de l'Institut français du Pétrole, 40(6), 755-784. https://doi.org/10.2516/ogst:1985045

Huang, W., Hersi, O.S., Lu, S. and Deng, S., 2017. Quantitative modelling of hydrocarbon expulsion and quality grading of tight oil lacustrine source rocks: Case study of Qingshankou 1 member, central depression, Southern Songliao Basin, China. Marine and Petroleum Geology, 84(1), 34-48. https://doi.org/10.1016/j.marpetgeo.2017.03.021

Li, J., Ma, W., Wang, Y., Wang, D., Xie, Z., Li, Z., Ma, C., 2018. Modeling of the whole hydrocarbon-generating process of sapropelic source rock. Petroleum Exploration & Development, 45(3), 461-471. https://doi.org/10.1016/S1876-3804(18)30051-X

Li, J., Wang, W., Cao, Q., Shi,Y., Yan, X., Tian, S., 2015. Impact of hydrocarbon expulsion efficiency of continental shale upon shale oil accumulations in eastern China. Marine and Petroleum Geology, 59(1), 467-479. https://doi.org/10.1016/j.marpetgeo.2014.10.002

Jin, H. and Sonnenberg, S.A., 2013. Characterization for source rock potential of the Bakken Shales in the Williston Basin, North Dakota and Montana. Unconventional Resources Technology Conference. Society of Exploration Geophysicists, American Association of Petroleum 12-14. August 2017. https://doi.org/10.1190/urtec2013-013

Kamali, M.R. and Mirshady, A.A., 2004. Total organic carbon content determined from well logs using ΔLogR and Neuro Fuzzy techniques. Journal of Petroleum Science and Engineering, 45(3-4), 141-148. https://doi.org/10.1016/j.petrol.2004.08.005

Lafargue, E., Espitalie, J., Jacobsen, T. and Eggen, S., 1990. Experimental simulation of hydrocarbon expulsion. Organic Geochemistry, 16(1-3), 121-131. https://doi.org/10.1016/0146-6380(90)90032-U

Lafargue, E., Marquis, F. and Pillot, D., 1998. Rock-Eval 6 applications in hydrocarbon exploration, production, and soil contamination studies; Les applications de rock-eval 6 dans lexploration et la production des hydrocarbures, et dans les etudes de contamination des sols. Revue de lInstitut Francais du Petrole, 53(4), 421-437. https://doi.org/10.2516/ogst:1998036

Lafargue, W., Espitalie, J., Broks, T.M. and Nyland, B., 1994. Experimental simulation of primary migration. Organic Geochemistry, 22(3-5), 575-586. https://doi.org/10.1016/0146-6380(94)90126-0

Landais, P., Michels, R. and Elie, M., 1994. Are time and temperature the only constraints to the simulation of organic matter maturation? Organic Geochemistry, 22(3-5), 617-630. https://doi.org/10.1016/0146-6380(94)90128-7

Langford, F. and Blanc-Valleron, M.-M., 1990. Interpreting Rock-Eval pyrolysis data using graphs of pyrolizable hydrocarbons vs. total organic carbon (1). AAPG Bulletin, 74(6), 799-804. DOI:10.1306/0C9B238F-1710-11D7-8645000102C1865D

Lehne, E. and Dieckmann, V., 2007. Bulk kinetic parameters and structural moieties of asphaltenes and kerogens from a sulphur-rich source rock sequence and related petroleums. Organic Geochemistry, 38(10), 1657-1679. https://doi.org/10.1016/j.orggeochem.2007.06.006

Lewan, M.D., 1997. Experiments on the role of water in petroleum formation. Geochimica et Cosmochimica Acta, 61(17), 3691-3723. DOI： 10.1016/s0016-7037(97)00176-2

Lewan, M.D., Dolan, M.P. and Curtis, J.B., 2014. Effects of smectite on the oil-expulsion efficiency of the Kreyenhagen Shale, San Joaquin Basin, California, based on hydrous-pyrolysis experiments. AAPG bulletin, 98(6), 1091-1109. DOI: 10.1306/10091313059

Leythaeuser, D., Mackenzie, A., Schaefer, R.G. and Bjoroy, M., 1984. A novel approach for recognition and quantification of hydrocarbon migration effects in shale-sandstone sequences. AAPG Bulletin, 68(2), 196-219. https://doi.org/10.1306/AD4609FE-16F7-11D7-8645000102C1865D

Leythaeuser, D., Schaefer, R.G. and Radke, M., 1987. SP2 on the primary migration of petroleum, 12th World Petroleum Congress. World Petroleum Congress 26. April 1987.

Li, C., Pang, X., Huo, Z., Wang, E. and Xue, N., 2020. A revised method for reconstructing the hydrocarbon generation and expulsion history and evaluating the hydrocarbon resource potential: Example from the first member of the Qingshankou Formation in the Northern Songliao Basin, Northeast China. Marine and Petroleum Geology, 121(1), 104577. https://doi.org/10.1016/j.marpetgeo.2020.104577

Li, R., Jin, K. and Lehrmann, D.J., 2008. Hydrocarbon potential of Pennsylvanian coal in Bohai Gulf Basin, Eastern China, as revealed by hydrous pyrolysis. International Journal of Coal Geology, 73(1), 88-97. https://doi.org/10.1016/j.coal.2007.07.006

Li, Y., Wang, X., Wu, B., Li, G. and Wang, D., 2016. Sedimentary facies of marine shale gas formations in Southern China: The Lower Silurian Longmaxi Formation in the southern Sichuan Basin. Journal of Earth Science, 27(5), 807-822. DOI： 10.1007/s12583-015-0592-1

Liu, B., Wang, H., Fu, X., Bai, Y., Bai, L., Jia, M., He, B., 2019. Lithofacies and depositional setting of a highly prospective lacustrine shale oil succession from the Upper Cretaceous Qingshankou Formation in the Gulong sag, northern Songliao Basin, northeast China. AAPG Bulletin, 103(2), 405-432. DOI：10.1306/08031817416

Ma, W., Hou, L., Luo, X., Liu, J., Tao, S., Guan, P., Cai, Y., 2020. Generation and expulsion process of the Chang 7 oil shale in the Ordos Basin based on temperature-based semi-open pyrolysis: Implications for in-situ conversion process. Journal of Petroleum Science and Engineering, 190(1), 107035. https://doi.org/10.1016/j.petrol.2020.107035

Milliken, K.L., Zhang, T., Chen, J. and Ni, Y., 2020. Mineral Diagenetic Control of Expulsion Efficiency in Organic-rich Mudrocks, Bakken Formation (Devonian-Mississippian), Williston Basin, North Dakota, USA. Marine and Petroleum Geology. 127, 104869. https://doi.org/10.1016/j.marpetgeo.2020.104869Get rights and content

Wang, M., Lu, S., Xue, H., 2011. Kinetic simulation of hydrocarbon generation from lacustrine type I kerogen from the Songliao Basin: Model comparison and geological application. Marine and Petroleum Geology, 28(9), 1714-1726. https://doi.org/10.1016/j.marpetgeo.2011.07.004

Pan, S., Zou, C., Yang, Z., Dong, D., Wang, Y., Wang, S., Wu, S., Huang, J., Liu, Q., Wang, D., Wang, Z., 2015. Methods for shale gas play assessment: A comparison between Silurian Longmaxi shale and Mississippian Barnett shale. Journal of Earth Science, 26(2), 285-294. DOI：10.1007/s12583-015-0524-0

Pandey, B., Pathak, D.B., Mathur, N., Jaitly, A.K., Singh, A.K. and Singh, P.K., 2018. A preliminary evaluation on the prospects of hydrocarbon potential in the carbonaceous shales of Spiti and Chikkim formations, Tethys Himalaya, India. Journal of the Geological Society of India, 92(4), 427-434. DOI: 10.1007/s12594-018-1037-0

Jiang, Q., Wang, Y., Qin, J., Wang, Q., Zhang, C., 2010. Kinetics of the hydrocarbon generation process of marine source rocks in South China. Petroleum Exploration and Development, 37(2), 174-180. https://doi.org/10.1016/S1876-3804(10)60024-9

Rahman, M., Herod, A. and Kandiyoti, R., 2000. Correlation of the Rock-Eval hydrocarbon index with yields of pyrolysis oils and volatiles determined in a wire-mesh reactor. Fuel, 79(2), 201-205. https://doi.org/10.1016/S0016-2361(99)00143-X

Rullkötter, J., Leythaeuser, D., Horsfield, B., Littke, R., Mann, U., Müller, P.J., Radke, M., Schaefer, R.G., Schenk, H.-J., Schwochau, K., Witte, E.G., Welte, D.H., 1988. Organic matter maturation under the influence of a deep intrusive heat source: a natural experiment for quantitation of hydrocarbon generation and expulsion from a petroleum source rock (Toarcian shale, northern Germany). Organic Geochemistry, 13(4-6), 847-856. https://doi.org/10.1016/0146-6380(88)90237-9

Sandvik, E.L., Young, W.A. and Curry, D.J, 1992. Expulsion from hydrocarbon sources: the role of organic absorption. Organic Geochemistry, 19(1-3), 77-87. https://doi.org/10.1016/0146-6380(92)90028-V

Shi, M., Yu, B., Zhang, J., Huang, H., Yuan, Y., Li, B., 2018. Evolution of organic pores in marine shales undergoing thermocompression: A simulation experiment using hydrocarbon generation and expulsion. Journal of Natural Gas Science and Engineering, 59, 406-413. https://doi.org/10.1016/j.jngse.2018.09.008

Singh, M.P. & Singh, P. K 1994: Indications of Hydrocarbon generation in the coal deposits of the Rajmahal basin, Bihar: Revelation of Fluorescence microscopy. J. Geol. Soc. India, vol. 43, no.6, pp.647-658.

Singh, P.K., 2011. Geological and petrological considerations for coal bed methane exploration: A review. Energy Sources, Part A: Recovery, Utilization, and Environmental Effects, 33(13), 1211-1220. DOI: 10.1080/15567030903330678

Singh, P.K., Singh V.K., Rajak, P.K., Singh, M.P., Naik, A.S., Raju, S.V., Mohanty, D., 2016a. Eocene lignites from Cambay basin, Western India: An excellent source of hydrocarbon. Geoscience frontiers, 7(5), 811-819. https://doi.org/10.1016/j.gsf.2015.08.001

Singh, P.K., 2012. Petrological and geochemical considerations to predict oil potential of Rajpardi and Vastan lignite deposits of Gujarat, Western India. Journal of the Geological Society of India, 80(6), 759-770. DOI：10.1007/s12594-012-0206-9

Singh, P.K., Rajak, P.K., Singh, V.K., Singh, M.P., Naik, A.S., Raju, S.V., 2016b. Studies on thermal maturity and hydrocarbon potential of lignites of Bikaner–Nagaur basin, Rajasthan. Energy Exploration & Exploitation, 34(1), 140-157. https://doi.org/10.1177/0144598715623679

Singh, P.K., Singh, V.K., Rajak, P.K., Mathur, N., 2017a. A study on assessment of hydrocarbon potential of the lignite deposits of Saurashtra basin, Gujarat (Western India). International Journal of Coal Science & Technology, 4(4), 310-321. https://doi.org/10.1007/s40789-017-0186-x

Singh, V.P., Singh, B.D., Mathews, R.P., Singh, A., Mendhe, V.A., Singh, P.K., Mishra, S., Dutta, S., Shivanna, M., Singh, M.P., 2017b. Investigation on the lignite deposits of Surkha mine (Saurashtra Basin, Gujarat), western India: Their depositional history and hydrocarbon generation potential. International Journal of Coal Geology, 183(1), 78-99. https://doi.org/10.1016/j.coal.2017.09.016

Sweeney, J.J., Braun, R.L., Burnham, A.K., Talukdar, S. and Vallejos, C., 1995. Chemical kinetic model of hydrocarbon generation, expulsion, and destruction applied to the Maracaibo Basin, Venezuela. AAPG bulletin, 79(10), 1515-1531. https://doi.org/10.1306/7834DA26-1721-11D7-8645000102C1865D

Tissot, B.P., Welte, D.H., 2013. Petroleum formation and occurrence, second ed. Springer Science & Business Media, Berlin.

Ungerer, P., Burrus, J., Doligez, B., Chenet, P.Y. and Bessis, F., 1990. Basin evaluation by integrated two-dimensional modeling of heat transfer, fluid flow, hydrocarbon generation, and migration (1). AAPG Bulletin, 74(3), 309-335. https://doi.org/10.1306/0C9B22DB-1710-11D7-8645000102C1865D

Varma, A.K., Hazra, B., Mendhe, V.A., Chinara, I. and Dayal, A.M., 2015. Assessment of organic richness and hydrocarbon generation potential of Raniganj basin shales, West Bengal, India. Marine and Petroleum Geology, 59(1), 480-490. https://doi.org/10.1016/j.marpetgeo.2014.10.003

Wang, E., Liu, G., Pang, X., Li, C., Zhao, Z., Feng, Y., Wu, Z., 2020. An improved hydrocarbon generation potential method for quantifying hydrocarbon generation and expulsion characteristics with application example of Paleogene Shahejie Formation, Nanpu Sag, Bohai Bay Basin. Marine and Petroleum Geology, 112(1), 104106. https://doi.org/10.1016/j.marpetgeo.2019.104106

White, D.A. and Gehman, H.M., 1979. Methods of estimating oil and gas resources. AAPG Bulletin, 63(12), 2183-2192. https://doi.org/10.1306/2F918900-16CE-11D7-8645000102C1865D

Wu, Y., Ji, L., He, C., Zhang, Z., Zhang, M., Sun, L., Su, L., Xia, Y., 2016. The effects of pressure and hydrocarbon expulsion on hydrocarbon generation during hydrous pyrolysis of type-I kerogen in source rock. Journal of Natural Gas Science and Engineering, 34(1), 1215-1224. https://doi.org/10.1016/j.jngse.2016.08.017

Xie, X., Volkman, J.K., Qin, J., Borjigin, T., Bian, L., Zhen, L., 2014. Petrology and hydrocarbon potential of microalgal and macroalgal dominated oil shales from the Eocene Huadian Formation, NE China. International Journal of Coal Geology, 124(1), 36-47. http://dx.doi.org/10.1016/j.coal.2013.12.013

Zeng, F., Dong, C., Lin, C., Wu, Y., Tian, S., Zhang, X., Lin, J., 2021. Analyzing the effects of multi-scale pore systems on reservoir Properties—A case study on Xihu Depression, East China Sea Shelf Basin, China. Journal of Petroleum Science and Engineering, 203(1), 108609. https://doi.org/10.1016/j.petrol.2021.108609